



## Study of LFV in Tau Decay at Belle

T. Ohshima<sup>a</sup> for the Belle Collaboration

<sup>a</sup>Nagoya University, Physics department  
Chikusa-ku, Nagoya 464-8602, Japan

New results from Belle in the search for lepton flavor violation phenomena in tau-decay are presented. They are  $\tau \rightarrow \ell\gamma$ ,  $\ell(\eta/\eta'/\pi^0)$ ,  $\ell V^0$  and  $\ell K_s$  decays (where  $\ell = \mu/e$  and  $V^0 =$  neutral vector mesons), and have reached the upper limits of (a few - several)  $\times 10^{-8}$  in the branching fraction.

### 1. Introduction

Flavor mixing in the quark sector appears to be a common phenomenon, and is represented in terms of the CKM matrix. Analogical mixing is also found in the lepton sector by means of neutrino oscillations, and is represented in this case as the Maki-Nakagawa-Sakata matrix. How about charged lepton mixing? It could appear as LFV phenomena, if such mixing is allowed. LFV is forbidden in the standard theory, SM. Even though neutrinos have masses and mix with each other, their contribution to LFV is negligibly small due to the smallness of the neutrino mass and the GIM cancellation mechanism. For instance, the branching fraction of  $\tau \rightarrow \mu\gamma$  decay is expressed as

$$\begin{aligned} Br(\tau \rightarrow \mu\gamma) &= \frac{3\alpha}{32\pi} \sum_i \left| U_{\tau i} U_{\mu i}^* \frac{m_{\nu i}^2}{M_W^2} \right|^2 \\ &\simeq 0. \end{aligned} \quad (1)$$

Therefore, the detection of LFV is in itself a direct indication of new physics beyond the SM.

Since LFV depends on some powers of the lepton mass, the heaviest lepton, tau, provides a very good ground to search for New Physics beyond the SM. Many models predict possible LFV with relatively large branching fractions, as can be seen in Table 1, which could be reachable at a high-luminosity B factory, such as the KEKB-Belle experiment.

Flavor mixing will appear through the off diagonal elements of the mass matrix. In the SM, Higgs will produce them. For quark and lepton

Table 1

Branching fractions of, for instance,  $\tau \rightarrow \mu\gamma$  and  $\tau \rightarrow \ell\ell\ell$  predicted by models of new physics beyond the SM.

model	$Br(\tau \rightarrow \mu\gamma)$	$Br(\tau \rightarrow \ell\ell\ell)$
mSUGRA + seesaw	$10^{-7}$	$10^{-9}$
SUSY + SO(10)	$10^{-8}$	$10^{-10}$
SM + seesaw	$10^{-9}$	$10^{-10}$
Non-Universal Z'	$10^{-9}$	$10^{-8}$
SUSY + Higgs	$10^{-10}$	$10^{-7}$

masses,  $(m_f)_{ij} = Y_{ij}v$ , where  $Y_{ij}$  is the Yukawa coupling element and  $v$  is the vacuum expectation value. In SUSY, for the squark and slepton mass matrix,  $(m_f^2)_{ij} = (Y^\dagger Y)_{ij}v^2 + m_{ij}^2$ . The SUSY-breaking mass term (the second term) dominates the mass matrix and induces LFV. There are many models to explain what kind of physics induces this breaking mass term, such as GUT, a seesaw mechanism, leptogenesis, etc. Tau's LFV relates to the off-diagonal elements of  $m_{31}^2$  and  $m_{32}^2$ .

### 2. KEKB-Belle

Belle collaboration at the KEKB  $e^+e^-$  asymmetric-energy collider (3.5 GeV of  $e^+ \times 8$  GeV of  $e^-$ ) now successfully accumulates more than one billion tau decays in the  $e^+e^- \rightarrow \tau^+\tau^-$  reaction. It is two orders of magnitude larger than experiments of the previous era, such as what the

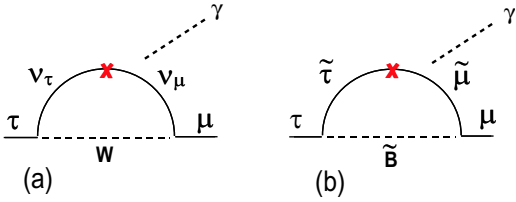


Figure 1.  $\tau \rightarrow \mu\gamma$  decay in (a) SM and (b) SUSY.

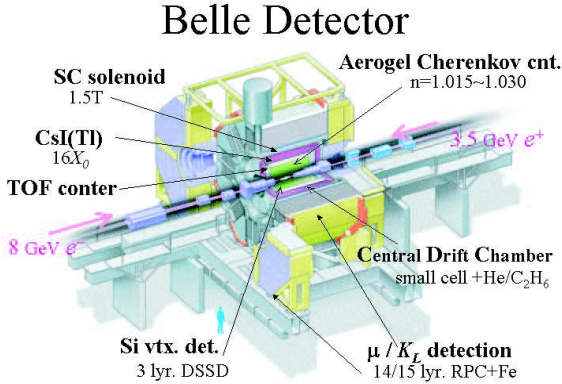


Figure 2. Schematic view of the Belle spectrometer.

CLEO collaboration attained. A brief description of the Belle spectrometer can be found in these Proceedings [1]; for details see [2].

## 2.1. Overview

### 2.1.1. Statistics and background

Data statistics, measurement resolution and the signal-to-background (BG) ratio play important roles to attain high sensitivity in the LFV search. Among them, the statistics is most essential, right now. When we get  $1,000 \text{ fb}^{-1}$  of data, a single-event sensitivity of  $1 \times 10^{-8}$  in terms of the branching fraction could be achieved with a detection efficiency of 5% in the case of no BG. We now have half of such an amount of data.

KEKB realizes a maximum luminosity of  $1.6 \times 10^{34} \text{ sec}^{-1} \text{ cm}^{-2}$  and Belle accumulates more than  $560 \text{ fb}^{-1}$  of data. With Belle's current schedule, two-times data, or 1 billion tau-pairs will be obtained next year, and 2 billion 3 years later. The Belle spectrometer has been steadily operated while showing good performance.

On the other hand, it is basically quite difficult to completely remove the backgrounds, since we always loose some kinematical information with neutrino(s) accompanying generic decay of the tag-side  $\tau$ .

### 2.1.2. Signal selection

To avoid repeating our description of signal selections in individual LFV searches, their common approaches are briefly mentioned here.

In our analysis, a single track is required at the tag-side with any number of photons. Single-prong decay occupies about 84% in tau decay. The signal-side comprises an objective LFV decay of an exclusive mode (see, Figure 3(a)). Although this criterion is simple, it is not a strong constraint for purely extracting signal candidates because neutrino(s) at the tag-side always carry information. Therefore, BG suppression is the most substantial issue in the analysis.

A relevant signal region is blinded to avoid any human bias until the last stage of signal selection.

At the last stage of signal selection, the number of signals is evaluated in the  $M_{\text{inv}}$  vs  $\Delta E$  plane.  $M_{\text{inv}}$  is the invariant mass of the candidate event, and  $\Delta E = E_{\text{sig}} - E_{\text{beam}}^{\text{CM}}$  is the energy difference between the candidate's energy and the beam energy in the center-of-mass frame. Therefore, signals should distribute around  $M_{\text{inv}} \simeq m_\tau$  and  $\Delta E = 0$ , as illustrated in Figure 3(b).

Figure 4 shows a so-selected event among several candidates found in our previous  $\tau \rightarrow \mu\gamma$  analysis [3]. It satisfies all of the criteria that we imposed as a  $\tau \rightarrow \mu\gamma$  decay, so that it cannot be further distinguished from BG. However, a detailed examination, not included in the analysis, let us suppose that it might be a radiative  $\mu\mu$  event, where one of the  $\mu$ 's comprises the  $\tau \rightarrow \mu\gamma$  signal conditions with a radiative photon, and the other  $\mu$  passes away close to a detector gap so that

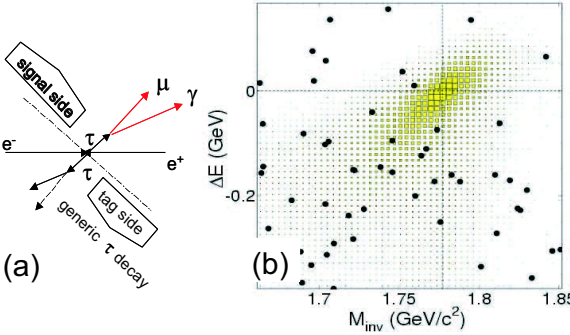


Figure 3. (a) signal configuration to be searched for in the analysis, and (b) candidate distribution in the  $M_{\text{inv}}$  vs  $\Delta E$  plane. As an example,  $\tau \rightarrow \mu\gamma$  case is illustrated [3].

it is misidentified as a particle, but not a  $\mu$  ( $\mu$ ).

In the analyses, Monte Carlo (MC) simulations play important roles to determine selection criteria and understand behaviors of data distributions. Programs to generate events of individual relating reactions, such as KORALB/TAUOLA for  $\tau$  decays, are mentioned in [1].

### 2.1.3. Upper-limit evaluation

Since we have not yet detected any significant amounts of signals, the result is expressed in terms of an upper limit on the branching fraction. There are two evaluation ways so far, which depend on the BG rate. For a small number of events around the signal region, counting methods, such as by Feldman and Cousins [4], Cousins and Highland [5], and Pole program [6], are applied. However, for a fairly large amount of events surviving around the signal region, a maximum likelihood fit is applied and an upper limit is evaluated by toy-MC [7].

Belle has observed 42 different LFV modes. Early analyses used only  $87 \text{ fb}^{-1}$  of data, but now it is more than  $500 \text{ fb}^{-1}$ . In the following section, we describe new measurements published this year.

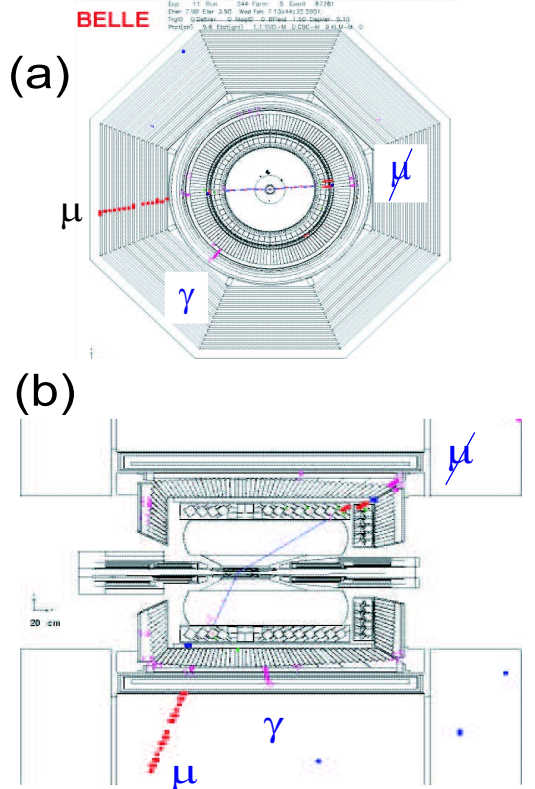


Figure 4. Event display of a  $\tau \rightarrow \mu\gamma$  candidate, selected in a previous search [3].

## 3. Belle Results

### 3.1. $\tau \rightarrow \mu\gamma$ and $e\gamma$

#### 3.1.1. $\tau \rightarrow \mu\gamma$

These decays are the most attractive LFV processes. Due to the heaviness of the tau mass, this branching fraction is generally remarked to be enhanced by a factor of  $10^{5-6}$  times that of the  $\mu \rightarrow e\gamma$  LFV.

MSSM with the seesaw model [8] predicts

$$\begin{aligned} Br(\tau \rightarrow \mu\gamma) &\sim 100 \times Br(\tau \rightarrow \mu ee), \\ Br(\tau \rightarrow \mu\gamma) &\sim 400 \times Br(\tau \rightarrow 3\mu). \end{aligned}$$

On the other hand, the left-right symmetric model [9] and the triplet Higgs for the neutrino mass [10] predict an opposite relation between

$Br(\tau \rightarrow \mu\gamma)$  and  $Br(\tau \rightarrow 3\mu)$ .

In MSSM with seesaw, the branching fraction of  $\tau \rightarrow \mu\gamma$  is estimated in terms of the ratio of the vacuum expectation values ( $\tan\beta$ ) and the SUSY-mass ( $M_{\text{SUSY}}$ ) in the case of  $\tan\beta > 1$ , as

$$Br(\tau \rightarrow \mu\gamma) = 3 \times 10^{-6} \left( \frac{\tan\beta}{60} \right)^2 \left( \frac{M_{\text{SUSY}}}{1 \text{ TeV}} \right)^{-4}. \quad (2)$$

## Backgrounds

A signal candidate is selected by looking for events containing exactly two opposite charged tracks and at least one photon,

$$\begin{aligned} e^+e^- &\rightarrow \tau^+\tau^- \\ &\rightarrow (\mu + \gamma) + \{(a \text{ track}) + n\gamma\}, \end{aligned} \quad (3)$$

where one  $\tau$  (signal-side) decays to  $\mu\gamma$  and the other (tag-side) decays to a non-muon charged particle ( $\mu$ ), any number of photons, and neutrino(s), as illustrated in Figure 3(a). The details can be found in [3].

In our previous analysis [3] where we used  $86 \text{ fb}^{-1}$  of data, the selection criteria successfully removed most of the BG's, but some that originated from  $\tau$ -pair and  $\mu$ -pair reactions with initial state radiation remained. In order to form a reliable probability density function of the BG distribution in a likelihood fit, we thoroughly studied the source and its behavior of BG's.

The  $\tau$ -pair with an initial radiation  $\gamma$  yields the largest contamination through a generic  $\tau \rightarrow \mu\nu\bar{\nu}$  decay of either  $\tau$ 's. Most of this BG is removed by introducing a cut on a relation between the missing mass-squared ( $m_{\text{miss}}^2$ ) and the missing momentum ( $p_{\text{miss}}$ ), as can be seen in Figure 5(a). The  $\mu$ -pair with an initial radiation  $\gamma$  makes the second-largest BG contribution, as described in the previous section:  $(\mu\gamma) + \mu$ . We avoided this BG by requiring the particle at the tag-side not to be a muon.

The BG from  $\tau$ -pair distributes mostly in the  $\Delta E < 0$  region. MC results are shown by an open histogram, data after opening the blind are indicated by points with errors, and an expected signal distribution is shown by a shadowed one in Figure 5(b). BG from the  $\mu$ -pair distributes not only in the negative, but also in the positive  $\Delta E$  region. The BG distribution in the  $M_{\text{inv}}-\Delta E$

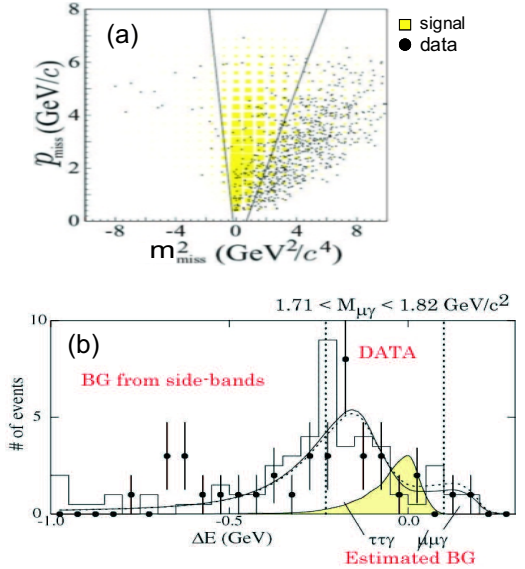


Figure 5. (a)  $m_{\text{miss}}^2$  vs  $p_{\text{miss}}$ , where BG's, mostly  $\tau\tau\gamma$  and  $\mu\mu\gamma$ , are removed by imposing a cut, indicated by lines. (b)  $\Delta E$  distribution after the selections, where BG's and signals by the MC simulation are indicated by the open histogram and shadowed area, respectively, and data are plotted by points with errors (the blind was opened). The solid curve is the sum of  $\tau\tau\gamma$  and  $\mu\mu\gamma$  estimated BG's.

plane was then expressed as the sum of above-mentioned two BG components. The solid curve in Figure 5(b) is the so-obtained  $\Delta E$  distribution for BG's.

Using the above-obtained BG and signal distributions, the BG's and signal's probability density functions, we applied an unbinned maximum likelihood method to extract the number of signals.

## New data

We now use  $535 \text{ fb}^{-1}$  of data, it is about a 6-times larger amount than the previous one. The analysis procedure is essentially the same as the previous one, but the selection conditions are tuned more carefully. As a result, the number of remaining events was 54 in the previous anal-

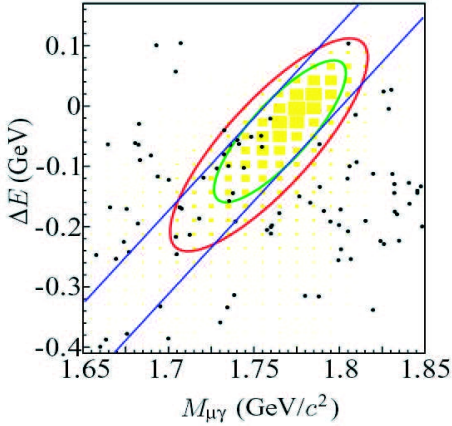


Figure 6.  $\tau \rightarrow \mu\gamma$  candidates survived from the selection. Data and MC signals are indicated by points and shadowed squares. Larger ellipse with  $\pm 3\sigma$ 's indicates the blinded region, and the smaller one with  $\pm 2\sigma$ 's the signal region used for evaluating the number of signals.

ysis, but it is 94 events this time over the same size of the box region ( $\pm 5\sigma_{M_{\text{inv}}} \times \pm 5\sigma_{\Delta E}$ , where  $\sigma$  is a resolution of  $M_{\text{inv}}$  or  $\Delta E$ ) in the  $M_{\text{inv}}\text{-}\Delta E$  plane.

The BG distribution is well-explained following our knowledge obtained previously. Remaining events are shown in Figure 6. Data and the signal MC are indicated by points and shadowed squares, respectively. The larger elliptic region with  $\pm 3\sigma$ 's indicates the blind area in the course of analysis. As can be seen, BG is less in the  $\Delta E > 0$  region and some dense population line is found around  $\Delta E \sim -0.2$  (GeV), which was also observed in the previous analysis. Accordingly, we exclude such a BG dense area from the signal region. An elliptic area with  $\pm 2\sigma$ 's is accordingly taken as the signal region. It provides a detection efficiency of  $\epsilon = 6.7\%$ .

An unbinned extended maximum likelihood fit [7] is applied to evaluate the number of signals, as

$$\mathcal{L} = \frac{e^{-(s+b)}}{N!} \prod_{i=1}^N (sS_i + bB_i), \quad (4)$$

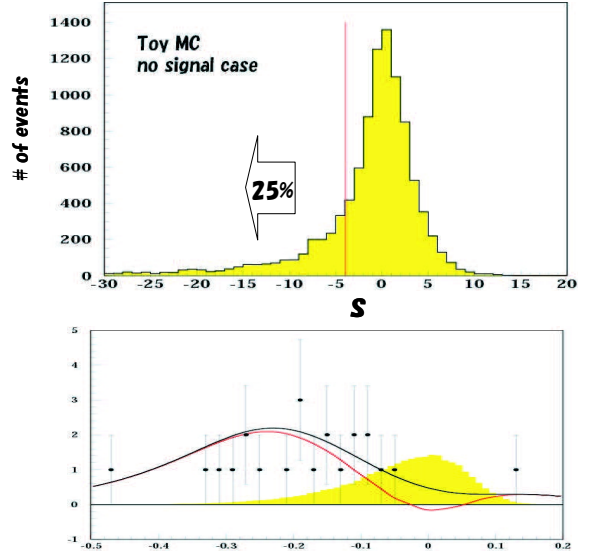


Figure 7. (a) Resulting  $s$  distribution by a toy MC in the case of no signal under our experimental conditions. (b) Projected data distribution and resulting fit.

where  $N$  is the number of observed events,  $s$  and  $b$  are free parameters representing the numbers of signal and BG events to be extracted, respectively, and  $S_i \equiv S(M_{\text{inv}}^{(i)}, \Delta E^{(i)})$  and  $B_i \equiv B(M_{\text{inv}}^{(i)}, \Delta E^{(i)})$  are the signal and BG probability density functions for  $i$ th events.

The resultant number of signals is  $s = -3.9$  events and  $b = 13.9$  events. Toy MC indicates that the probability to get signal events less than  $s = -3.9$  is 25% in the case of a null true signal (see, Figure 7(a)). To compare the event distribution with the fit result, for illustrative purposes we take a band, as shown by lines in Figure 6 along the long axis of the ellipse with a width of  $\pm 2\sigma$ , and project the distributions onto the long axis. Figure 7(b) is the so-obtained event distribution. The solid and dashed curves are BG and signal+BG, respectively, and the signal MC distribution is indicated by the shadowed area. Over most of the signal region, we do not find

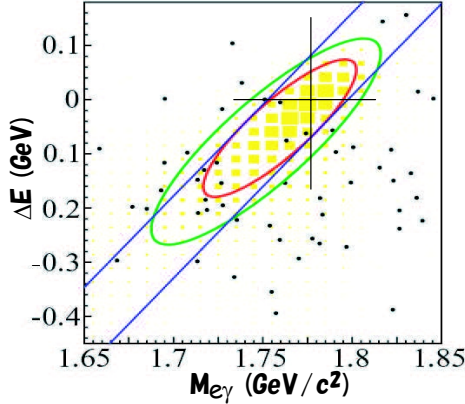


Figure 8.  $\tau \rightarrow e\gamma$  candidates survived from the selection. See the caption of Figure 6 for an explanatory note.

any event.

The resulting upper limit at the 90% C.L. is  $s_{90} = 2.0$  events. An upper limit on the branching fraction is obtained via the formula

$$\begin{aligned} Br(\tau \rightarrow \mu\gamma) &= \frac{s_{90}}{2\epsilon N_{\tau\tau}} \\ &= 4.5 \times 10^{-8}, \end{aligned} \quad (5)$$

where a total systematic error of 4.0% is included.

### 3.1.2. $\tau \rightarrow e\gamma$

Using the same strategy as  $\tau \rightarrow \mu\gamma$ ,  $e\gamma$  is also searched for. Within the  $\pm 2\sigma$  signal region, we find 5 events (Figure 8), compared to 10 events for  $\mu\gamma$ . The fit gives  $s = -0.14$  signal events and  $b = 5.14$  BG events. According to MC, there is a 48% probability to have  $s < -0.14$  events in the fit. As a result, the upper limit on the branching fraction at the 90% C.L. is

$$Br(\tau \rightarrow e\gamma) = 1.2 \times 10^{-7}. \quad (6)$$

## 3.2. $\tau \rightarrow (\mu/e) + (\eta/\eta'/\pi)$

### 3.2.1. $\tau \rightarrow \mu\eta$

The  $\tau \rightarrow \mu\eta$  decay is quite interesting: it can be mediated by a SUSY Higgs, which couples to the s-quark current (see, Figure 9). When it couples to the  $\mu$  current, it is the decay  $\tau \rightarrow 3\mu$ . Compared to  $3\mu$ ,  $\mu\eta$  is enhanced by a color factor of

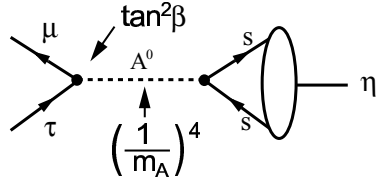


Figure 9.  $\tau \rightarrow \mu\eta$  LFV decay mediated by a SUSY Higgs.

3, mass-dependent Yukawa coupling, and phase space. It results in about a factor of 8. Some theories [11] predict a larger branching fraction of  $\mu\eta$  than  $\mu\gamma$ :  $Br(\tau \rightarrow \mu\eta)/Br(\tau \rightarrow \mu\gamma) \simeq 5$ . Among the decay modes discussed in this section,  $\mu\eta$  is expected to have the largest branching fraction, for instance,  $Br(\tau \rightarrow \mu\eta)/Br(\tau \rightarrow \mu\pi^0) \simeq 166$  and  $Br(\tau \rightarrow \mu\eta)/Br(\tau \rightarrow \mu\eta') \simeq 250$ .

In our previous analysis [12], we achieved an upper limit of  $Br(\tau \rightarrow \mu\eta) = 1.5 \times 10^{-7}$  at the 90% C.L. using  $154 \text{ fb}^{-1}$  of data. In both the previous and new analyses,  $\eta$  was reconstructed using the decay modes of  $\gamma\gamma$  and  $3\pi$ 's (see, Figure 10). BG's are from the  $\tau$ -pair and the  $q\bar{q}$  continuum. The selection criterion on the missing quantities between  $m_{\text{miss}}^2$  vs  $p_{\text{miss}}$  plays an important role to remove those BG's.

We now use  $401 \text{ fb}^{-1}$  of data, which is a 2.6-times larger amount than the previous one, and apply the same selection criteria, but they are finely tuned to more effectively remove BG's. Figure 11 shows the events survived from the selection in the  $M_{\text{inv}}$  vs  $\Delta E$  plane for the (a)  $\gamma\gamma$  and (b)  $3\pi$  modes, respectively. The ellipse is the signal region, determined to contain 90% of the signal MC events. The detection efficiency is  $\epsilon = 6.4\%$  and  $6.8\%$  for the  $\gamma\gamma$  and  $3\pi$  modes, respectively. While 0.4 or 0.2 events in the signal region are expected from the side-band event distribution, no event was found in both modes. Accordingly, the upper limit of the signal was evaluated to be 2.1 and 2.2 events for  $\gamma\gamma$  and  $3\pi$ , respectively. The combined upper limit on the branching fraction at the 90% C.L., including

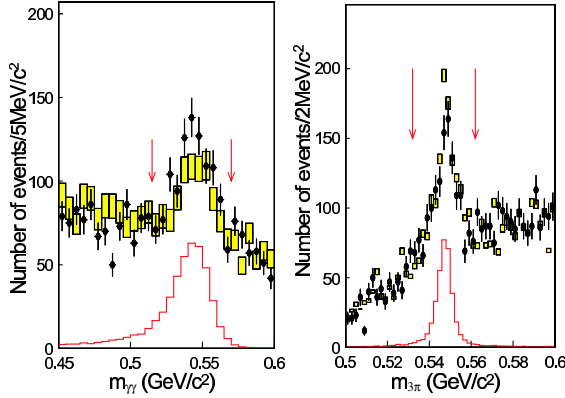


Figure 10. Invariant mass distribution of (a)  $\gamma\gamma$  and (b)  $3\pi$  in new analysis. Data and MC are indicated by points and shadowed squares, respectively.

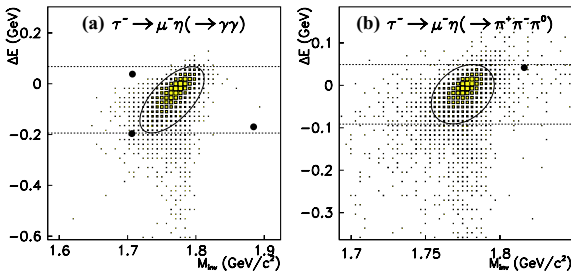


Figure 11.  $\tau \rightarrow \mu\eta$  candidates in  $M_{\text{inv}}$  vs  $\Delta E$  for (a)  $\eta \rightarrow \gamma\gamma$  and (b)  $\eta \rightarrow 3\pi$  modes. Data and signal MC events are indicated by points and shadowed squares, respectively, and the ellipse is the signal region.

systematic uncertainties, is

$$Br(\tau \rightarrow \mu\eta) = 6.5 \times 10^{-8}. \quad (7)$$

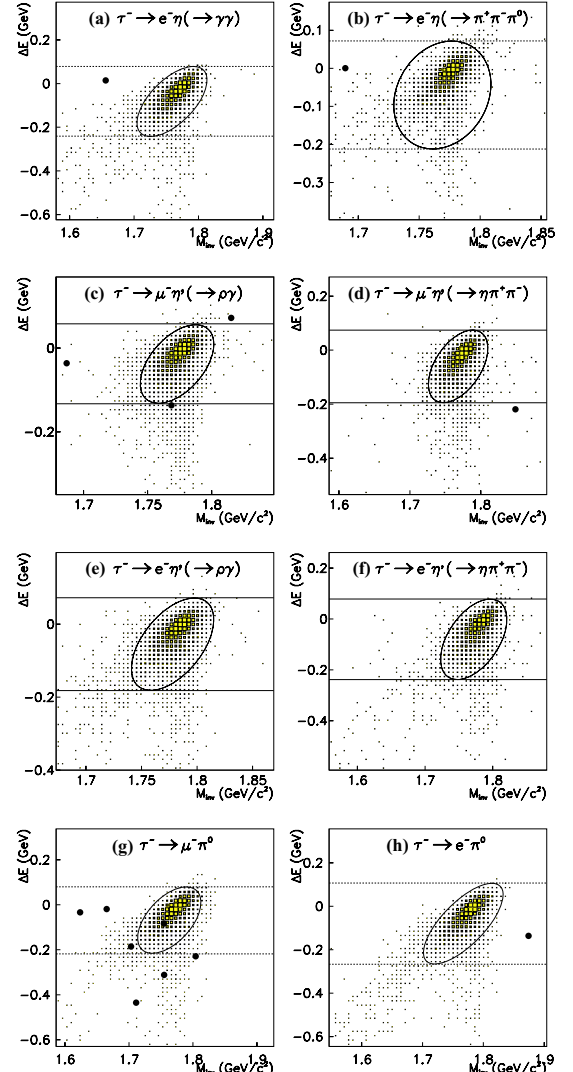


Figure 12. Event distributions in  $M_{\text{inv}}-\Delta E$  after the selection for (a)  $\tau \rightarrow e\eta (\rightarrow \gamma\gamma)$ , (b)  $e\eta (\rightarrow 3\pi)$ , (c)  $\mu\eta' (\rightarrow \rho\gamma)$ , (d)  $\mu\eta' (\rightarrow \eta\pi\pi)$ , (e)  $e\eta' (\rightarrow \rho\gamma)$ , (f)  $e\eta' (\rightarrow \eta\pi\pi)$ , (g)  $\mu\pi^0 (\rightarrow \gamma\gamma)$  and (h)  $e\pi^0 (\rightarrow \gamma\gamma)$ .

### 3.2.2. $\tau \rightarrow e\eta$ and $(\mu/e) + (\eta'/\pi^0)$

Five other similar LFV decays ( $\tau \rightarrow e\eta$ ,  $\mu\eta'$ ,  $e\eta'$ ,  $\mu\pi^0$  and  $e\pi^0$ ) were also searched for using a similar approach with  $\tau \rightarrow \mu\eta$ . The essential dif-

Table 2

Summary of analyses for  $\tau \rightarrow e\eta$ ,  $(\mu/e)\eta'$  and  $(\mu/e)\pi^0$  decays.  $n(\text{exp})$  and  $n(\text{obs})$  are the number of expected and observed events, respectively, in the signal region.

mode	$e\eta$	$\mu\eta'$		$e\eta'$	$\mu\pi^0$	$e\pi^0$
$\eta/\eta'/\pi^0 \rightarrow$	$3\pi$	$\gamma\gamma$	$\pi\pi\eta$	$\rho\gamma$	$\pi\pi\eta$	$\rho\gamma$
$\epsilon$ (%)	4.7	4.6	4.9	5.4	4.3	4.8
$n(\text{exp})$	0.53	0.25	0	0.23	0	0
$n(\text{obs})$	0	0	0	0	0	1
$UL @90\%CL$	2.0	2.2	2.5	2.2	2.5	3.8
$Br(\times 10^{-8})$	26	17	41	19	47	25
combined $Br(\times 10^{-8})$	9.2		13		16	

ference from our previous analysis with  $154 \text{ fb}^{-1}$  of data is in  $\eta'$  selection: the  $\eta' \rightarrow \rho\gamma$  decay mode is included to enlarge the detection efficiency of  $\tau \rightarrow (\mu/e)\eta'$ .

Figure 12 shows the event distributions in the  $M_{\text{inv}}-\Delta E$  plane after the selection. Very few events survive the selections;  $\mu\pi^0$  exhibits the largest amounts, only six in  $\pm 10\sigma$ 's box size. A MC study suggests them to have originated from  $\tau \rightarrow \rho\nu$  decay.

Table 2 compares the expected and observed number of events in the signal region. The upper limits of the signals were obtained using Pole program [6], and their branching fractions are expressed in terms of the upper limit at the 90% C.L. as

$$\begin{aligned} Br(\tau \rightarrow e\eta) &= 9.2 \times 10^{-8}, \\ Br(\tau \rightarrow \mu\eta') &= 13 \times 10^{-8}, \\ Br(\tau \rightarrow e\eta') &= 16 \times 10^{-8}, \\ Br(\tau \rightarrow \mu\pi^0) &= 12 \times 10^{-8}, \\ Br(\tau \rightarrow e\pi^0) &= 8 \times 10^{-8} \end{aligned} \quad (8)$$

### 3.3. $\tau \rightarrow (\mu/e) + (\text{hh or a vector-meson})$

Decays to a lepton ( $\ell = \mu/e$ ) plus two hadrons ( $\pi^\pm, K^\pm$ ), or a neutral vector-meson ( $V^0$ ), such as  $\rho^0(\rightarrow \pi^+\pi^-)$ ,  $\phi(\rightarrow K^+K^-)$ ,  $K^{*0}(\rightarrow K^\pm\pi^\mp)$ , are searched for using  $158 \text{ fb}^{-1}$  of data [13]. The final states comprise three charged tracks. We then look for those events in which the signal hemisphere contains a lepton and 2 opposite-

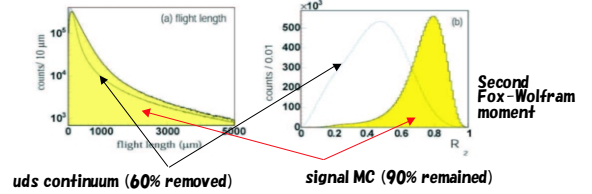


Figure 13. (a) Flight length and (b) the second Fox-Wolfram moment distributions for the signal (shaded) and  $uds$  continuum (open) MC events.

charged tracks, and in the other hemisphere for a lepton and any number of photons.

Mass constraint on  $V^0$  effectively helps to remove BG's in  $\tau \rightarrow \ell V^0$ . BG sources are  $\tau$ -pair and  $q\bar{q}$  for  $\mu V^0$ , and  $\tau$ -pair and 2-photon process for  $eV^0$ . To exclude BG's, a two-dimensional likelihood ratio by means of the  $\tau$ 's flight length and the second Fox-Wolfram moment is employed, as can be seen in Figure 13; 60% of the continuum is removed, while 90% of the signals remain by demanding the ratio to be larger than  $\mathcal{L}_{\text{sig}}/(\mathcal{L}_{\text{sig}} + \mathcal{L}_{uds}) > 0.45$ , where  $\mathcal{L}_{\text{sig}}$  and  $\mathcal{L}_{uds}$  are the likelihood probabilities for the signal and  $uds$  continuum, respectively.

The final event distributions in the  $M_{\text{inv}}-\Delta E$  are shown in Figure 14(a) and (b) for  $\ell hh$  and

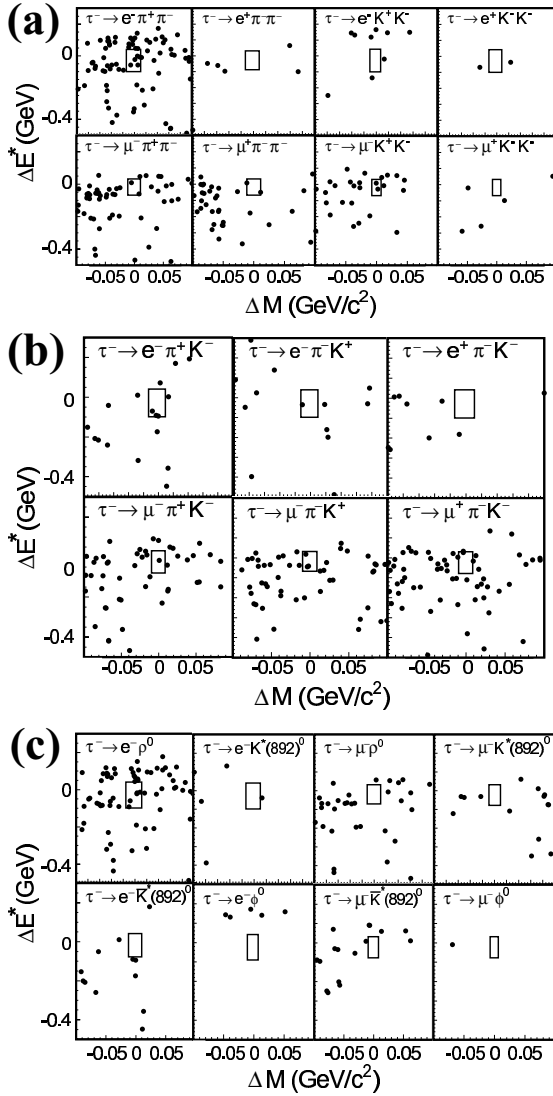


Figure 14. Event distributions in  $M_{\text{inv}} - \Delta E$ , for  $\tau \rightarrow \ell hh$ , (a) and (b), and  $\tau \rightarrow \ell V^0$ , (c). The box indicates the 90% signal region.

Figure 14(c) for  $\ell V^0$ .

We look for 14 modes in  $\tau \rightarrow \ell hh$ , and 8 modes in  $\tau \rightarrow \ell V^0$ . Resulted upper limits on the branching fraction are also listed in Table 3: they range over  $Br = 2 - 8 \times 10^{-7}$  at the 90% C.L.

Table 3

Summary of  $\tau \rightarrow \ell hh$  and  $\ell V^0$  searches. UL means the upper limit of the branching fraction, multiplied by a factor of  $10^7$ ;  $\epsilon$  is the detection efficiency; “exp” and “obs” are the expected and observed number of events in the signal region, respectively.

mode	UL	$\epsilon(\%)$	exp	obs
$e^- \pi^+ \pi^-$	7.3	5.30	$2.6 \pm 1.1$	6
$e^+ \pi^- \pi^-$	2.0	5.14	$0.0 \pm 0.3$	1
$\mu^- \pi^+ \pi^-$	4.8	4.4	$0.8 \pm 0.3$	2
$\mu^+ \pi^- \pi^-$	3.4	4.4	$0.7 \pm 0.3$	1
$e^- \pi^+ K^-$	7.2	4.0	$0.9 \pm 0.3$	3
$e^- \pi^- K^+$	1.6	4.1	$1.3 \pm 0.4$	0
$e^+ \pi^- K^-$	1.9	4.0	$0.7 \pm 0.2$	0
$e^- K^- K^+$	3.0	3.1	$0.3 \pm 0.2$	0
$e^+ K^- K^-$	3.1	3.1	$0.1 \pm 0.1$	0
$\mu^- \pi^+ K^-$	2.7	3.4	$2.3 \pm 0.4$	1
$\mu^- \pi^- K^+$	7.3	3.3	$1.9 \pm 0.3$	3
$\mu^+ \pi^- K^-$	2.9	3.5	$2.5 \pm 0.4$	1
$\mu^- K^- K^+$	8.0	2.8	$0.5 \pm 0.2$	2
$\mu^+ K^- K^-$	4.4	2.7	$0.1 \pm 0.1$	0
$e^- \rho^0$	6.5	5.0	$2.6 \pm 1.0$	5
$e^- K^{*0}(892)$	3.0	4.1	$0.8 \pm 0.3$	0
$e^- \bar{K}^{*0}(892)$	4.0	3.7	$0.2 \pm 0.1$	0
$e^- \phi$	7.3	2.9	$0.04 \pm 0.04$	0
$\mu^- \rho^0$	2.0	4.4	$0.3 \pm 0.1$	0
$\mu^- K^{*0}(892)$	3.9	3.6	$0.4 \pm 0.1$	0
$\mu^- \bar{K}^{*0}(892)$	4.0	3.4	$0.5 \pm 0.2$	0
$\mu^- \phi$	7.7	2.7	$0.0 \pm 0.2$	0

### 3.4. $\tau \rightarrow (\mu/e) + K_s$

The last one is the decay of  $\tau \rightarrow \ell K_s$  [14]. We now use  $281 \text{ fb}^{-1}$  of data. The selection criteria are similar to that in previous searches for  $\tau \rightarrow \ell hh$ , but a reconstruction of  $K_s$  from two hadrons, having a decay vertex away from the interaction point and a narrow invariant mass, helps reject BG’s. BG comes from D decays to  $\ell K_s \nu$  and  $\pi K_s$ , but their contributions are suppressed to a negligible level. In this analysis we newly introduce a powerful selection criterion on the relation between the momentum of the  $\ell K_s$  system and the opening angle between the  $\ell$  and  $K_s$ , as can be seen in Figure 15.

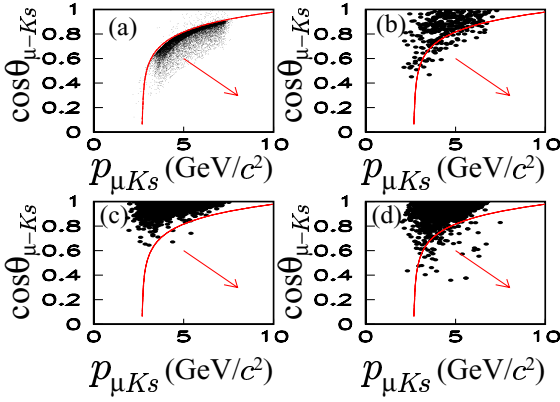


Figure 15.  $\cos\theta_{\mu-K_s}$  vs  $p_{\mu K_s}$  distributions of (a) signal MC, (b)  $q\bar{q}$  MC, (c)  $\tau\tau$  MC, and (d) data. The selected area is indicated by a curve.

We find a few events around the signal region. For both modes, no event is observed in the signal region, while 0.2 event is expected, with a detection efficiency of  $\epsilon = 13.5\%$  and  $11.8\%$  for  $\mu K_s$  and  $e K_s$ , respectively (see Figure 16). The resulting branching fraction with systematic errors is

$$\begin{aligned} Br(\tau \rightarrow \mu K_s) &= 4.9 \times 10^{-8}, \\ Br(\tau \rightarrow e K_s) &= 5.6 \times 10^{-8}, \end{aligned} \quad (9)$$

at the 90% C.L. These sensitivities improve the previous CLEO measurement [15] by a factor of  $\sim 20$ .

#### 4. Summary and Discussions

KEKB-Belle now provides more than  $500 \text{ fb}^{-1}$  of data, which corresponds to about 1 billion  $\tau$ -decays. It is a two orders of magnitudes larger statistical amount than in the previous era's experiment, mostly performed at CLEO.

LFV searches at the Belle collaboration have greatly progressed in proportion to its data. While PDG lists up to 51 LFV modes, we have examined 42 LFV modes until now, as can be seen in Figure 17. It now reaches a sensitivity of  $\mathcal{O}(10^{-8})$  on the branching fraction: it is improved by about 100 times compared to the pre-

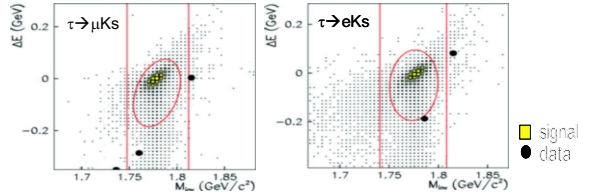


Figure 16. Resultant event distributions in  $M_{\text{inv}}$  vs  $\Delta E$  for (a)  $\tau \rightarrow \mu K_s$  and (b)  $\tau \rightarrow e K_s$ . Data are indicated by points, and the signal region by an ellipse. The region put between the vertical lines is blinded during selections.

vious era. Unfortunately, no signal event has been found in any decay mode. Therefore, these results contribute to the search for New Physics by constraining the possible parameter space of the models.

For instance, our new data of  $Br(\tau \rightarrow \mu\gamma) < 4.5 \times 10^{-8}$  excludes a large area of the predicted possible  $Br(\tau \rightarrow \mu\gamma)$  vs.  $m_{\tau_1}$  region, and also imposes a constraint on the relation between  $\tan\beta$  and  $M_{\text{SUSY}}$ , following eq.(2), as can be seen in Figure 18. Similarly, our  $Br(\tau \rightarrow \mu\eta) < 6.5 \times 10^{-8}$  excludes a large  $\tan\beta$  region with a relatively small  $m_A$  area, following eq.(5), as shown in Figure 19. Those constraints on the parameter spaces are obtained under certain typical conditions for many SUSY variables. We are now in a position to carry out a more systematic study about the impact on the new physics, based on our new data over a variety of 42 LFV decay modes.

At the time of 2003 Aachen EPS meeting, we just reached the upper limit of  $Br(\tau \rightarrow \mu\gamma) = 1 \times 10^{-6}$ ; after 3 years, we now attain  $Br(\tau \rightarrow \mu\gamma) = 4.5 \times 10^{-8}$ . The progress is quite rapid. How much sensitivity can we achieve within the next few years?

We will accumulate  $1,000 \text{ fb}^{-1}$  of data, 2-times larger than what we currently have, next years. In 2009, hopefully  $2,000 \text{ fb}^{-1}$ , 4 times. Can we reach beyond the  $Br = \mathcal{O}(10^{-8})$  level? It depends not only on the data statistics, but also the BG rate.

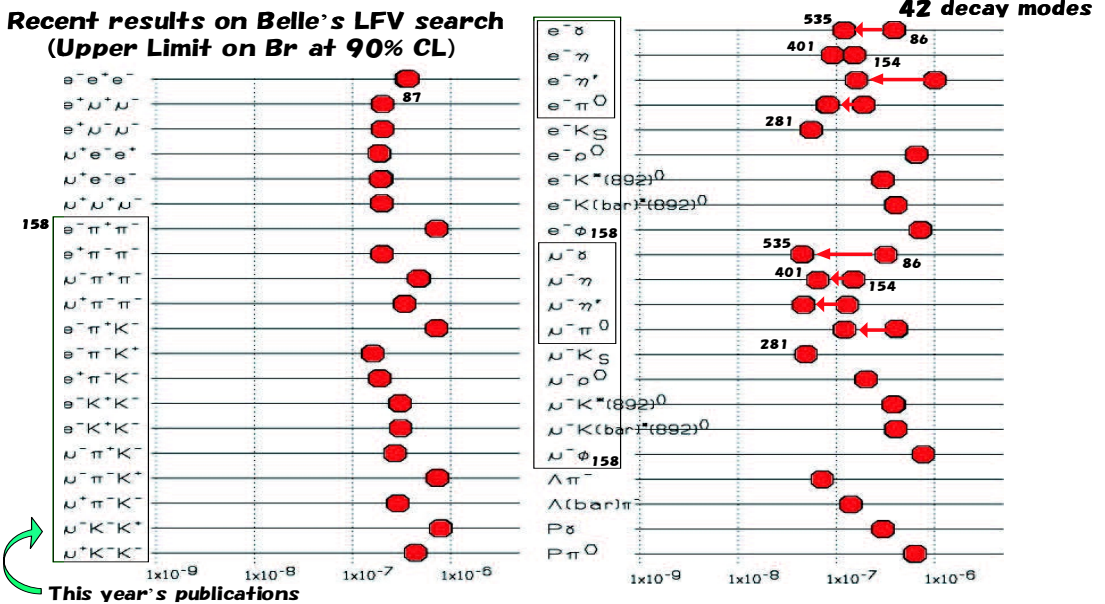


Figure 17. Belle's LFV search results. 42 LFV modes have been studied, and the resulting upper limits are indicated by points. The modes included in the box are the measurements published this year. The small numbers next to the points or boxes are the data luminosities used in the analysis.

Figure 20 is the expected sensitivity on  $\tau \rightarrow \mu\gamma$ , also prepared for the Aache meeting, by a Toy MC, assuming the BG condition realized at the first of our analysis. The MC result is plotted by triangles. When BG is proportional to the luminosity ( $\mathcal{L}$ ), the sensitivity will have  $\propto 1/\sqrt{\mathcal{L}}$  behavior. On the other hand, if no BG exists, it behaves as  $\propto 1/\mathcal{L}$ .

Our new result deviates from the expectation. This is partly due to our improved method of analysis, and partly due to the statistical fluctuation.

As an example,  $\tau \rightarrow \mu\gamma$  has non-negligible BG contributions. Thus, the sensitivity will not be improved much with increasing luminosity, but rather proportional to  $1/\sqrt{\mathcal{L}}$ . Even if we accumulate a twice amount of data, about 1,000  $\text{fb}^{-1}$ , the achievable sensitivity will be around  $Br(\tau \rightarrow \mu\gamma) = 3 \times 10^{-8}$ . On the other hand, such as  $\tau \rightarrow \mu\eta$  and  $\mu K_s$  will have very few BG events, even with 1,000  $\text{fb}^{-1}$ , so that their sensitivities will achieve  $Br \sim 2 \times 10^{-8}$ . We are

requested to reduce BG further by exploring the analysis method. Thus, within a few years, some of the modes will go into the  $\mathcal{O}(10^{-9})$  level, we hope. That is a very interesting task for our tau society.

## REFERENCES

1. T. Ohshima, “First measurement of  $\tau \rightarrow \phi K\nu$  by Belle”, these Proceedings.
2. A. Abashian *et al.*, Belle Collaboration, Nucl. Instrum. Meth., A 479, (2002) 117.
3. K. Abe *et al.*, Belle Collaboration, Phys. Rev. Lett. 92, (2004) 171802.
4. G. J. Feldman and R. D. Cousins, Phys. Rev. D 57, (1998) 3873.
5. R. D. Cousins and V. L. Highland, Nucl. Instrum. Methods, A 320, (1992) 331;
6. J. Conrad *et al.*, Phys. Rev. D 67 (2003) 012002.
7. I. V. Narsky, Nucl. Instrum. Methods, A 450 (2000) 444.
8. For instance, J. Hisano *et al.*, Phys. Lett. B 357, (1995) 579; S. F. King and M. Oliveira, Phys.

- Rev. D 60, (1999) 035003.
9. K. S. Babu, B. Dutta and R. N. Mohapatra, Phys. Lett. B 458, (1999) 93.
  10. E. Ma, Nucl. Phys. Proc. Suppl. 123, (2003) 125.
  11. M. Sher, Phys. Rev. D 66, (2002) 057301; A. Brignole and A. Rossi, Nucl. Phys. B 701, (2004) 3.
  12. Y. Enari *et al.*, Phys. Lett. B 622, (2005) 218.
  13. Y. Yusa em et al., Phys. Lett. B 640, (2006) 138.
  14. Y. Miyazaki *et al.*, Phys. Lett. B 639, (2006) 159.
  15. S. Chen *et al.*, CLEO Collabpration, Phys. Rev. D 66, (2002) 072201.
  16. J. R. Ellis *et al.*, Phys. Rev. D 66 (2002) 115013.

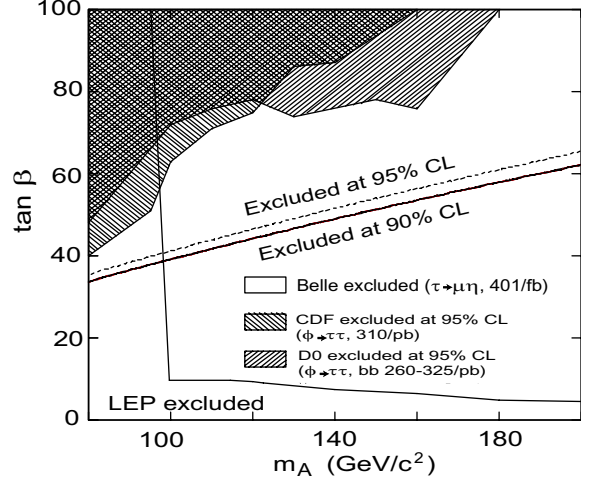


Figure 19. An excluded region on the relation between  $\tan \beta$  and  $m_A$  by our new data, following eq(5).

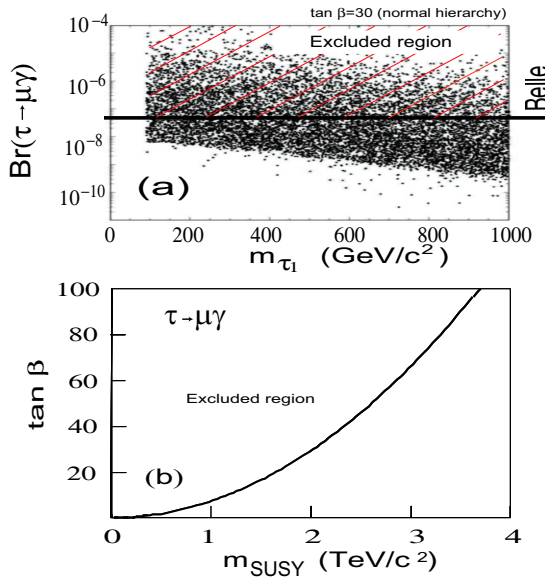


Figure 18. (a) Prediction on  $Br(\tau \rightarrow \mu\gamma)$  by [16] and our new result. (b) an excluded region on  $\tan \beta$  vs  $M_{\text{SUSY}}$ , imposed by eq.(2)

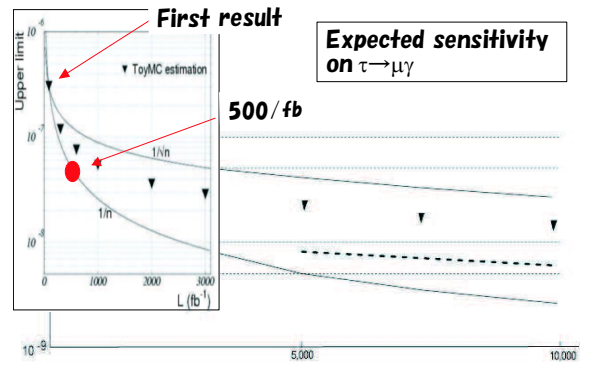


Figure 20. The expected sensitivity of  $Br(\tau \rightarrow \mu\gamma)$  as a function of luminosity.